Japan Geoscience Union Meeting 2013
(May 19-24 2013 at Makuhari, Chiba, Japan)

SSS28-P01 Room:Convention Hall Time:May 23 18:15-19:30

Fault plane heterogeneity determined by fractal geometry of fault zones

Kenshiro Otsuki[1*]

[1]Dept. Geol., Graduate School of Science, Tohoku Univ.

Investigation 1

Fault planes are inherently heterogeneous and this is a source of variety of earthquakes. Fault zones are composed of fault segments and jogs. Otsuki & Dilov (2005, JGR, 110, B03303) found for experimentally made fault zones of 1 mm order lengths that fault segments + jogs structures are hierarchically self-similar. With the additional data of small geological faults of a 10 m order length scale and strike-slip seismic faults longer than the thickness of seismogenic layer which emerged on the earth's surface, segment length $L_S(i)$, jog length $L_J(i)$ and jog width $W_J(i)$ show the correlations below,

$L_S(i+1) = 0.348\ L_S(i)^{0.994}$ approx. $L_S(i+1) = 0.365\ L_S(i)$ —— (1)

$W_J(i) = 0.0278\ L_S(i)^{1.06}$ approx. $W_J(i) = 0.0402\ L_S(i)$ —— (2)

$W_J(i) = 0.191\ L_J(i)^{0.990}$ approx. $W_J(i) = 0.189\ L_J(i)$ ——— (3),

where i denotes the hierarchical rank. These relations indicate the fractal dimension D of fault zone geometry is close to 2.

For the individual three data set eqs. (2) and (3) are represented by $W_J(i) = b\ L_S(i)^H$, $W_J(i) = a\ L_J(i)^A$ with different proportional constants and power values.

For experimental faults..... b=0.00385, H=0.642, a=0.00694, A=0.516.
For geologic small faults..... b=0.333, H=0.763, a=0.141, A=0.558.
For strike-slip surface faults.. b=0.164, H=0.853, a=3.18, A=0.665.

Investigation 2

Seismologists have searched for appropriate distribution patterns of the heterogeneity which can explain the G-R law and the k^{-2} falloffs of earthquake displacement spectra (e.g. Madariaga, 1979, JGR, 84, 2243; Andrews, 1980, JGR, 85, 3867; Frankel, 1991, JGR, 96, 6291; Herrero & Bernard, 1994, BSSA, 84, 1216). They reached the conclusion that D is 2 if static stress drop is constant. This is very consistent with the analytical results for fault zone geometry mentioned above. The parameter H corresponds with the Hurst exponent, and it is related with D by D=E+1-H, where E denotes Euclidean dimension. Since H=0.853 for strike-slip seismic surface faults, D=2.15. Mai & Beroza (2002, JGR, 107, B11,2308) analyzed the slip distributions which were depicted by waveform inversions for many earthquakes, and found that D=2.29 and H=0.75 at an average, being consistent with my results.

Investigation 3

Mai & Beroza (2002, JGR, 107, B11,2308) estimated for correlation distances of slip distributions on fault planes to be about 1/3 of the effective fault lengths. Bersenev (2001, JGR, 28, 35) found that earthquakes are associated with sub-events with about 1/3 length scale of the main phases. These are consistent with eq. (1). It depicts that one overall fault zone is divided into three first-order segments, and that the fractal of fault plane geometry is not continuous but discrete (hierarchical). This discreteness is supported by the numerical simulations by Ben-Zion & Rice (1995, JGR, 100, 12959) in which real complex slip patterns were realized especially when strong and abrupt heterogeneities (of jogs) were assumed.

Investigation 4

Scholz (1982, BSSA, 72, 1) proposed that mean strike-slips are proportional to fault lengths even if the fault is much longer than the thickness of seismogenic layer (L-model). This curious problem has been open to discussion. My analytical results show that mean strike-slips U_m of surface large faults are related with fault lengths L_0 by the power function as,

$U_m = 0.246 {L_0}^{0.46}$ ——— (4).

Note that the power value is less than 1. This is caused by jogs which pin the fault slip to make faults stiffer. Only ${L_0}^{0.46}$ is interpreted to work as an fault length effective for slips. Recent numerical simulation results for seismic slips on heterogeneous fault planes (e.g. Hillers & Wesnousky, 2008, BSSA, 98, 1085; Dieterich & Smith, 2009, PAGEOPH, 166, 1799) realize such phenomena.

The relation with fracture surface energy and the evolution of fault zone geometry will be discuss elsewhere.

Keywords: fault plane, geometry, fractal, heterogeneity

Japan Geoscience Union Meeting 2013
(May 19-24 2013 at Makuhari, Chiba, Japan)

SSS28-P02 Room:Convention Hall Time:May 23 18:15-19:30

Numerical simulations for interactions of dynamic rupture on fault step-over

Keisuke Kanano[1*], Shoichi Yoshioka[2]

[1]Dept. of Earth and Planetary Sci., Kobe Univ, [2]RCUSS, Kobe Univ

Fault system on the Earth's surface consists of some segments with various structures such as bending, branching, and stepping. A part of stepping faults overlaps each other in many cases. In this study, we investigate interaction of dynamic rupture between two or more parallel planar vertical strike slip faults, and rupture stop in an overlapped zone, by spontaneous fault rupture simulations.

We used staggerd-grid split-node method (Dalguer and Day , 2007). As for the friction law, we assumed slip-weakening relationship. The initial stress field is assumed to be uniform, and elastic modulus is homogeneous. Assuming the three-dimensional orthogonal coordinate system, x axis is taken parallel to a fault plane, y axis is perpendicular to the fault, and z axis is taken downward(Earth's surface is z= 0 km). A fault is located in spatial range of -15 km<x<15 km, y= 0 km, and 0 km<z<15 km.This fault is hereafter referred to as Fault 1.The initial rupture zone is set in the central part of Fault 1. The second fault, which is Fault 2, is located in spatial range of -15 km<x<35 km and 0 km<z<15 km, changing the distance between the two faults in the y direction. Left lateral-strike slip faults were assumed, and extensional step was considered.

As a result, dynamic rupture of Fault 2 was triggered at the point located at the edge of Fault 1 (near x= 15 km) in all cases. After rupture was triggered on Fault 2, the rupture spread on the fault plane. In the overlapped zone, however, rupture on Fault 2 stopped spontaneously. This can be interpreted that shear stress drop in the overlapped zone on Fault 2 took place due to slip on Fault 1, causing difficulty for shear stress to reach strength on Fault 2. Simulated results for changing distance between the two faults showed that the smaller the distance is, the easier rupture stops in the overlapped zone on Fault 2, whereas the longer the distance is, the more difficult rupture stops on Fault 2. This is because the smaller the distance between the two faults is, the more the effect of shear stress drop by slip of Fault 1 on causing rupture on Fault 2 is large in the overlapped zone, whereas the larger the distance between the two faults is, the smaller the effect is. However, if the distance between the two faults is larger than a certain value, rupture on Fault 2 itself was not triggered anymore.

Keywords: step-over, spontaneous rupture simulation, rupture stop, staggerd-grid split-node method

Japan Geoscience Union Meeting 2013
(May 19-24 2013 at Makuhari, Chiba, Japan)

SSS28-P03 Room:Convention Hall Time:May 23 18:15-19:30

Slip stabilization, a counterintuitive slip response to a sudden buildup of loading stress, predicted by a revised rate

Nobuki Kame[1*], Satoshi Fujita[1], Masao Nakatani[1], Tetsuya Kusakabe[1]

[1]Earthquake Res. Inst., Univ. of Tokyo

Motivated by the existing discrepancies between the model predictions of Dieterich (1994) and the observed aftershock seismicity, we re-examined aftershock triggering on faults obeying the recently revised RSF incorporated with a newly noticed stress-weakening effect (Nagata et al., 2012) that seems eventually free from contradictions with laboratory friction experiments. Time-to-instability analysis, which is necessary as a specific nucleation model to get on the original theoretical framework of Dieterich's aftershock modeling, was numerically conducted to derive the resultant aftershock sequences obeying the revised RSF. It was found that certain improvements towards common observations, in terms of raised seismicity and shortened delay before Omori decay. However, the improvements were far too small to resolve the huge quantitative gap in the characteristic stress (direct effect coefficient 'a' times 'normal stress') between laboratory values and what is inferred from observed aftershock sequences. On the other hand, through many numerical simulations of slip response to a stress step imposed at different timings in the seismic cycle, we noticed a counterintuitive behavior of the revised RSF. When a sufficiently large stress step is imposed at a timing somewhat before entering self-accelerating stage of the seismic cycle, the timing of earthquake can be delayed rather than advanced. In this case, the earthquake will occur after several oscillatory cycles resembling slow slip events, which might be usable as a marker for a fault at a certain stage in the seismic cycle. This behavior itself is a potentially important finding in earthquake mechanics and a laboratory confirmation of the counterintuitive response of a frictional fault to a stress step, which is an unintended prediction by the revised RSF, is desired in the near future.

Reference

Kame, N., Fujita, S., Nakatani, M. and Kusakabe, T., Effects of a revised rate- and state-dependent friction law on aftershock triggering model, Tectonophysics (2012), http://dx.doi.org/10.1016/j.tecto.2012.11.028

Japan Geoscience Union Meeting 2013
(May 19-24 2013 at Makuhari, Chiba, Japan)

SSS28-P04 Room:Convention Hall Time:May 23 18:15-19:30

Dependence of earthquake stress drop on scaling of frictional parameters

Shingo Yoshida[1*], Naoyuki Kato[1]

[1]ERI, Univ. Tokyo

To understand dependence of stress drop on scaling of frictional parameters, we conducted numerical simulation of earthquake cycles on plate interface. We assume a circular asperity which obeys a rate- and state-dependent friction law. If the critical slip length L is proportional to the asperity radius r, and b-a is a constant, stress drop is independent of the ruptured area size R. On the other hand, if L is a constant independent of r, stress drop decreases with increasing R because earthquake occurs before large stress is accumulated compared with the former case. Numerical simulation shows the stress drop is proportional to Rˆ[-0.43]. Such a phenomenon is not observed for natural earthquakes. Kato (2012) reported that stress drop is proportional to Rˆ[-0.5] on the basis of 2-d simulation results and theory of fracture mechanics if fracture energy is independent of asperity size.

Keywords: stress drop, scaling, rate- and state-dependent friction law, asperity

Japan Geoscience Union Meeting 2013
(May 19-24 2013 at Makuhari, Chiba, Japan)

SSS28-P05 Room:Convention Hall Time:May 23 18:15-19:30

Complicated recurrence of slip events on a uniform circular asperity

Naoyuki Kato[1*]

[1]Earthquake Research Institute, University of Tokyo

Numerical simulation of repeated occurrence of slip events on a fault patch (asperity) is conducted to understand the mechanism of irregular sequence of slip events. The fault is uniformly shear loaded at a constant rate, and frictional stress acting on the fault is assumed to obey a rate- and state-dependent friction (RSF) law. A circular patch with velocity-weakening frictional property is embedded in a fault with velocity-strengthening frictional property elsewhere. A numerical simulation is conducted by varying the characteristic slip distance L of the RSF law. Slip behavior changes as L increases. When L is small, seismic slip events (earthquakes) repeatedly occur at a constant time interval. As L increases, recurrence of slip events becomes complex. Period doubled slip pattern, where seismic and aseismic slip events alternately occur, multiperiodic pattern, and aperiodic patterns occur. At the same time, slip tends to be aseismic with increasing L. The distributions of shear stress on the fault before the slip events are variable because of variations of the residual stress in the preceding slip event and aseismic sliding during an interseismic period. This variation in shear stress causes the complex sequence of slip events. Iteration maps of the recurrence intervals of slip events are examined by taking a plot of Ti versus Ti+1, where Ti denotes the time interval between the ith and (i+1)th slip events. Each iteration map for aperiodic sequence of slip events is expressed by a simple curve, suggesting that the occurrence time of the next event is predictable from the previous time interval and the slip event sequence exhibits deterministic chaos. To compare the simulation result of sequence of slip events on a velocity-weakening patch embedded in a velocity-strengthening region, a numerical simulation of slip on a velocity-weakening patch enclosed by unbreakable barrier. In this case, no complex recurrence of slip events is observed. When L is smaller than a critical value, seismic slip events repeatedly occur at a constant interval. On the other hand, stable sliding occurs when L is larger than the critical value. This result indicates that the complex slip behavior for a velocity-weakening patch embedded in a velocity-strengthening region comes from the interaction between the velocity-weakening and velocity-strengthening regions.

Keywords: earthquake cycle, asperity, chaos, simulation, friction

Japan Geoscience Union Meeting 2013
(May 19-24 2013 at Makuhari, Chiba, Japan)

SSS28-P06 Room:Convention Hall Time:May 23 18:15-19:30

Earthquake forecasting system based on sequential data assimilation of the slip on the plate boundary

Takane Hori[1*], Shin'ichi Miyazaki[2], Mamoru Hyodo[1], Ryoko Nakata[1], Yoshiyuki Kaneda[1]

[1]Japan Agency for Marine-Earth Science and Technology, [2]Graduate School of Science, Kyoto Univerisy

We are constructing an earthquake forecasting system based on sequential data assimilation of the slip on the plate boundary. We use SIS, a kind of particle filter for the data assimilation. The forward calculation is done using earthquake generation cycle simulation. From the simulation results, we estimate crustal deformation that can be compared to the observation of GEONET on land and DONET on the seafloor. We demonstrate numerical test of this system using synthetic data of seafloor deformation before virtual Tonankai or Nankai earthquakes. We also use real data set of GEONET to compare the results of earthquake generation cycles.

Japan Geoscience Union Meeting 2013
(May 19-24 2013 at Makuhari, Chiba, Japan)

SSS28-P07 Room:Convention Hall Time:May 23 18:15-19:30

A hypothesis of a super subevent associated with the 2011 Mw9.0 Tohoku Earthquake

Ichiro Kawasaki[1*], Hiroshi Ishii[1], Yasuhiro Asai[1]

[1]Tono Research Institute of Earthquake Science

Kawasaki et al. (2012) proposed a rectangle fault model for the 2011 Mw9.0 Tohoku earthquake to match the synthetic waveforms by the exact solution in a half space of Okada (1980) to overall features of the GPS high sampling data of GEONET and continuos stress recording at TOS, Toki, Gifu prefecture, of TRIES. One of their conclusions was that rupture of maim fault started 40 s after the origin time of JMA. However, since their model did not elucidate transverse component of GPS displacements especially remarkable in the south Kanto district, we reanalyze the data.

Fig.1 shows records sections of the transverse component of GPS data (black) and synthetic waveforms (red) by the main fault of Kawasaki et al. (2012) in three directions of N90W, N125W and N145W. A horizontal axis is arrival time of S waves as reduced by the S wave velocity of 3.8 km/s. Fig.1 means that the remarkable pulse between broken lines at 70 s and 95 s of the pulse width of 25 s to 30 s and the amplitude of up to 70 cm was SH waves propagating at the S wave velocity. Fig.1 also suggests that corresponding source was within or close to the main rupture area.

Since a low angle thrusting dipping to the west does not radiate SH waves to the west and radiate only small amplitude SH waves to the south, the source of the SH waves is supposed to be a subevent having a separate fault plane in which strike slip component is dominant.

Since a node of the SH wave polarity lies in an N80W direction, a strike direction of the subevent should be around N60E or N150E. Starting from initial model of vertical left lateral strike slip fault above the plate boundary, we attempt trial and error approach to propose the following rectangle subfault model: strike direction N145E, dip angle 85, slip angle 85, origin time 20 s after the initiation of main fault, depth 40km, fault length 30 km, width 20 km, rupture propagation velocity of 3.0 km/s to the southwest and upward, rise time 15 s, dislocation 200 m and seismic moment 5.3x1021 Nm (Mw8.4). This subevent elucidates characteristic features of the SH waves at many GPS stations and the stress record at TOS. The SH phase is within wavetrains due to the main rupture and thus ambiguity of the fault parameters is large. However, for the pulse width of 25 s to 30 s and the large amplitude of up to 70 cm, we are sure that the dislocation was extraordinary large compared with a fault size. In this sense, we would like to call it a super subevent.

Fig.1 Record sections of the transverse component of the GPS high sampling data (black) obtained at the time of the 2011 Tohoku earthquake in three directions of N90W, N125W and N145W. Red traces are synthetic waveforms by a main fault model of Kawasaki et al. (2012) and the half space calculation of Okada (1980). A vertical axis is displacement in meter. Vertical spacing is arbitrary. A horizontal axis is a travel time reduced by S wave velocity of 3.8 km/s, assuming the JMA origin time and epicenter.

Keywords: 2011 Tohoku earthquake, subevent, GPS high sampling data, Continuous stress records, dislocation velocity

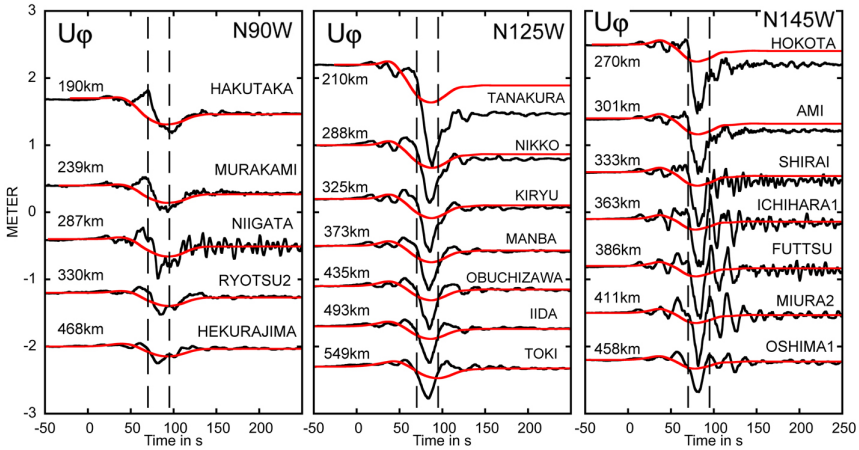

Japan Geoscience Union Meeting 2013
(May 19-24 2013 at Makuhari, Chiba, Japan)

SSS28-P08 Room:Convention Hall Time:May 23 18:15-19:30

Earthquake Energy Generation of Mw9 East Japan Off 2011

Shozaburo Nagumo[1*]

[1]Earthquake Research Institute, University of Tokyo

1. Purpose of the article

What on earth happened there, the Mw9.0 huge earthquake of East Japan off 2011. We present here a view. Firstly, the huge energy generation of Mw9 was done by the volume source, not by the plane source. Secondly, the huge energy-generation of Mw9 is a large-scale stress-adjustment activity, not the asperity rupture. The reasons are based on such observational facts as listed below.

2. Indicative features of volume source

(2-1) 3 big seismic-wave radiations. (2-2) The long duration time of seismic wave radiation. (2-3) The huge source area. (200km x 500km). (2-4) The oceanic mantle seismic activation (OBS observation)

3. Mechanism of volume source generation

Why it is a volume source? The theory of elasticity says that the seismic wave generation is the body force generation and the elastic strain-energy release. The earthquake source volume is the 3D region in which seismic waves are generated. Therefore body forces generate seismic waves. And the body forces are generated by vanishing elastic strain inside. One cause is due to the sudden crash of pores-and-cracks, and the other is due to the sudden change of the confining pressure. This is the generation of earthquake as well as volume source.

Because the geological rock body is regarded as a porous-cracked elastic body, and it is under the initial stresses of gravity and tectonic stresses. And the incremental stresses accumulate around the pores-and-cracks in long years..

4. Mechanism of the large-scale volume source generation

Why such a large-scale volume source is generated? The potential is the tectonic forces of the island-arc oceanic-trench system itself. Firstly, under the inclined surface, horizontal forces are generated towards the trench axis caused by the gradient of the self-weight pressure. Secondly, in the neighborhood of the trench, some upward and downward forces may be generated, probably metamorphism origin such as surpentinization and eclogite. Moreover, in the arc-side of the trench, the island-arc rock masses overload the underlying oceanic mantle. Thus, such forces generate a large-scale flexure and buckling deformations of the oceanic lithosphere. The buckling deformation leads to the elastic instability (Biot, 1965, Incremental Deformations). The scale of the instability is very large, more than several hundred km horizontally, more than 50km in depth including the overlying crust.

Its associated stress-distribution in such a broad region is block-wisely heterogeneous because of the tectonic history. Around the block boundaries, stresses concentrate and accumulate in long years. Thus the stress imbalance could exist broadly in the lithosphere of the island-arc and oceanic-trench system. Once the buckling fractures occur somewhere, these stresses could be successively released. This is the generation of the large earthquake and the large-scale volume source.

5. Process of stress-adjustment activity

How the huge area (200km x 500km) turned to the source area? At the beginning, a certain buckling fracture took place in the oceanic lithosphere, where the degree of deformations is high. The buckling fracture extended into the earth's crust leading to the detachment of rock-blocks. Then, the block-wise detachment released the confining pressure, and the rock masses were subjected to collapse, fracture and crash. These processes could correspond to the first 2 big seismic wave radiations in the northern part.

During these processes, the rock bodies loose its rigidity and are led to the fluidization, and caused the rock-flows. Such rock-flows are the shape deformation so as to decreases the gravity potential. The outward spreading rock-flow causes forces at the front as well as side-wards. Such a force might lead to the 3^{rd} big seismic wave radiation in the southern part. Such processes

as above are the large-scale stress-adjustment activity to level the stress imbalance in a broad region. These processes are not the asperity rupture.

Japan Geoscience Union Meeting 2013
(May 19-24 2013 at Makuhari, Chiba, Japan)

SSS28-P09 Room:Convention Hall Time:May 23 18:15-19:30

Model that harmonizes with the rupture process of (Ide et al.2011)–Relation between 3.11 and off-Miyagi-earthquakes–

Hirofumi Mase[1*]

[1]none

I presented the model concerning the cutting plane that expresses the range from the coast to Japan Trench off Miyagi and passes the epicenter of the 3.11 Tohoku-Oki Earthquake. I formed with clay the wedge to a above plate, the subducting plate and the one located below it to a lower. I did the experiment pushing from right and left by the same power after they had been overlapped. The slip of the plate boundary started in the depth, and the Front of Slip rose aiming at the shallow. Afterwards, ”Slip all together” of the entire boundary was generated because the shallow tip peeled off at a dash suddenly. I thought that the model had reproduced the feature off Miyagi and the process to 3.11 in 1,000 years.(above(1)) I also analyzed 42 remarkable past earthquakes in and around (2). I value (3) for the slip distribution and the rupture process of 3.11. I expect that the model will harmonize with (3) and past observation facts.

I clarified A) B) by the experiment afterwards. A)”Slip all together” is that the slip starts from ”Hypocenter” and spreads to both the depth and the shallow. B)The deepest portion of the above plate started crushing the slope of the lower rather than slipping up. I placed a released paper between the plate boundary. Bigness and smallness in that effect influenced the passage of time to ”Slip all together” and the overall amount of slip when ending. The event stagnates or ends imperfectly if the lower plate doesn’t subduct smoothly beneath the above plate in the depth.

I was able to read C) from (3). I set straight line L of 50km or more in length that Onagawa-cho is made a starting point and expands to the south almost and reaches north latitude 38th parallel. C)In the change chart of time of slip velocity(40,60,75sec), the north and the south are excluded, the spread was dammed up once by the line L, and slip seems to have happened in the deepest portion at a dash afterwards(90sec) (3).

A) is the maximum result expected and it harmonizes with (3). B) and C) harmonize. Therefore, it can be said, the straight line that passes the middle point of the line L and the epicenter of 3.11 is ”Center axis” of the compression system off Miyagi.

Though I explained the mechanics of the Earthquakes off Miyagi(EOFM), I interpreted for them to have happened usually because the Standoff before ”Slip all together” had continued long in (1)experiment (2). However, there is the following facts. (a)The Standoff was able to be shortened easily B). (b)Slip in the depth that came off from the hypocenters of EOFM after 1936 was large (3). (c)[1936M7.4][1937M7.1][1978M7.4][2005M7.2][2005M6.6][2010M5.5] approach the epicenter of 3.11 almost in order of generation along ”Center axis” (4)(2).

The row of hypocenters of (c) is not corresponding to the plate interface (2), and the distance has been still left for the hypocenter of 3.11 in addition. However, because a main shock extends within the considerable range and many aftershocks are accompanied usually, they(c) have the possibility of peeling off the boundary forward much and, needless to say, destroying the vicinity of theirself-hypocenter. Aren’t EOFM synonymous with the progress of the Front of Slip ?

(1)[Mase]http://jglobal.jst.go.jp/public/20090422/201202271822634851
(2)[Mase]http://homepage3.nifty.com/hmase/upload120927web.htm
(3)[Ide]http://www.s.u-tokyo.ac.jp/ja/press/2011/12.html
(4)[JMA]http://www.seisvol.kishou.go.jp/eq/gaikyo/monthly

Japan Geoscience Union Meeting 2013
(May 19-24 2013 at Makuhari, Chiba, Japan)

SSS28-P10 Room:Convention Hall Time:May 23 18:15-19:30

Development of Complex Seismic Source Inversion Method: Application to December 7, 2012 Sanriku-oki Earthquake

Amato Kasahara[1*], Yuji Yagi[1]

[1]Life and Env. Sci., Univ. of Tsukuba

Good knowledge of the seismic source process is important for understanding the stress regime and physical properties in and around the seismic source area. However, it is difficult to directly observe the co-seismic behavior on a fault in the interior of the Earth. Hence, many seismic source inversion methods have been developed, since the pioneering study of Trifunac (1974), to estimate the seismic source process using geophysical observations available on the earth's surface, under the assumption that the seismic energy was released by a hypothetical fault plane. Usually a simple planar fault is assumed and its geometry is decided from one of the nodal planes of the corresponding Centroid Moment Tensor (CMT) solution. However, it is well known that surface traces of faults are bending and branching; moreover, the complexity in fault geometry is also supported by the existence of earthquakes whose focal mechanism solution, determined using P-wave first-motion polarities, is different from their CMT solution and events for which the CMT solution contains large Compensated Linear Vector Dipole components.

Inversion with inappropriate fault geometry could result in a biased solution and increase the risk of misinterpretation. To mitigate the problem, it is better to estimate not only the seismic source process but also the fault geometry at the same time.

We developed a seismic source inversion method that does not require prior information of detailed fault geometry. In this approach, the seismic rupture process is formulated as a moment release function in a volume around the seismic source and the fault location is represented as a region of high moment release density within the rock volume.

First, we performed a synthetic test for the new method. In the test, both mechanism solution distribution and moment release were well recovered through the method. Next, we applied the method to real data from an earthquake occurred on Dec 7, 2012 at Far East of Honshu, Japan. We found that both a thrust type and a normal type earthquake occurred closely in space and time. The earthquake ruptured mainly two patches, one was a reverse faulting patch in deeper part, east of the hypocenter, the other was a normal faulting patch in the shallow part, west of the hypocenter. The normal faulting patch extended down to about 40 km, which is consistent with the deepest normal faulting events observed after the 2011 Tohoku earthquake in the region (Obana et al., 2012). The hypocenter was located between the reverse faulting patch and the normal faulting patch, where the stress state seems to be approximately neutral. The rupture seems to have propagated bidirectionally from the hypocenter towards both the reverse and normal faulting regions.

Keywords: source process, inversion, December 7, 2012 Sanriku-oki earthquake

Japan Geoscience Union Meeting 2013
(May 19-24 2013 at Makuhari, Chiba, Japan)

SSS28-P11 Room:Convention Hall Time:May 23 18:15-19:30

Source mechanism of the eastern Mino earthquake (Mj 5.1) with Isochron Backprojection Method

Makoto OKUBO[1*], Atsushi Saiga[1]

[1]TRIES, ADEP

An earthquake (eastern mino earthquake; Mj 5.1) has occurred beneath the high density seismogram networks (HDSN; cf. Aoki *et al.* 1999 and Okubo, 2011) that consisted with more than 50 stations among 30km x 20km area on the 14th Dec. 2011. This earthquake had normal faulting type mechanism in subducting philipine sea slub (Saiga and Okubo, reviewing). Seismic motion of this earthquake includes high frequency components (Okubo and Saiga, 2012; JPGU), we can resolve detailed rupture process using with the dense seismogram networks and the high frequency phenomena.

In order to analyze rupture process of the eastern mino earthquake, we applied isochron backprojection method (IBM; eg. Festa and Zollo, 2006, Pulido *et al.*, 2008). We used the waveform records of our stations and some Hi-net (Obara *et al.*, 2002) observatories within 65 km hypocentral distances as datasets of IBM. First, we picked up S wave arrival time from waveforms, and calculated acceleration amplitudes. And we estimated the S wave velocity structure around the epicenter from Matsubara *et al.* (2008) with Vp/Vs = 1.73 assumption. And also we assume that rupture velosity does not beyond the S wave velocity and the maximum rupture length does not extend above the Matsuda's fault length-Magnitude relation (Matsuda, 1975), in IBM analysis.

We will discuss rupture process of the eastern mino earthquake and relations with aftershock hypocenters distribution, in presentation.

Keywords: source mechanism, main rupture, s waveform, dense seimometer array, high frequency seismic motion

Japan Geoscience Union Meeting 2013
(May 19-24 2013 at Makuhari, Chiba, Japan)

SSS28-P12 Room:Convention Hall Time:May 23 18:15-19:30

A deep revers outer-rise earthquake triggered a shallow normal outer-rise earthquake - The 2012 Off-Sanriku earthquake -

Tomoya Harada[1*], Satoko Murotani[1], Kenji Satake[1]

[1]Earthquake Research Institute, the University of Tokyo

The Dec. 7, 2012 Off-Sanriku outer-rise earthquake (Mj7.4) had two successive sub-events, the first sub-event was a deep reverse event (Event 1) and the second one was a shallow normal event (Event 2), as revealed by the teleseismic body-wave analysis (Kikuchi and Kanamori, 2003). The estimated coseismic slip distributions show that Event 1 had a relatively simple circular slip distribution and Event 2 had two large slips. Calculated static changes in the Coulomb Failure Function (dCFF) due to Event 1 shows positive values around the Event 2' s rupture area, indicating that Event 2 was induced by Event 1.

After the 2011 Tohoku earthquake of M 9.0, many outer-rise earthquakes have occurred near the Japan Trench and the Dec. 7, 2012 Off-Sanriku (Mj 7.4) was one of such outer-rise events. In this study, we estimated mechanism solution for this event by using the Kikuchi and Knanamori (2003)'s teleseismic body-wave analysis programs. We used UD-component of P-waveforms recorded at 73 stations with distance from 30 to 90 degree and assumed two triangles as source time functions. The result shows that the 2012 Off-Sanriku earthquake had two successive sub-events, the first event was a deep reverse event (Event 1; depth: 56 km, strike: 171.8 deg., dip: 57.3 deg., rake: 68.5 deg.) and the second event was a shallow normal event and it took place 20 sec. later at 20 km from Event 1 in the N25deg.E direction (Event 2; depth: 6 km, strike: 23.7 deg., dip: 76.3 deg., rake: -94.5 deg.). Seismic moments of Event 1 and 2 are 5.9∗10^19 Nm (Mw7.1) and 7.8∗10^19 Nm (Mw7.2), respectively, and 8.8∗10^19 Nm (Mw7.2) in total. According to the Quick CMT Catalog, the reverse earthquake of Mw7.2 occurred at 144.09 deg. E, 38.01deg. N, and 58 km in depth, and normal earthquake of Mw7.2 followed 12 sec. after at 143.83 deg. E, 37.77 deg. N and 20 km in depth.

We then estimated coseismic slip distributions of Event 1 and 2 by the teleseismic body-wave inversion. The mechanism solutions and the point source locations estimated in the previous analysis were used for the initial mechanism and the rupture points, respectively, of both events. The coseismic slip of Event 1 is concentrated around the initial rupture point, with the maximum slip and average slip of 2.52 m and 0.43 m, respectively. As for Event 2, we used the residual waveforms that the synthetic waveforms from the slip distribution of Event 1 are subtracted from the observed waveforms. The slip distribution has two large slips. The maximum slip and average slip are 2.35 m and 0.82 m, respectively.

Finally, we calculated the static changes in the Coulomb Failure Function (dCFF) due to Event 1's slip distribution on steep nodal plane by using the Okada (1992)'s program. The positive dCFF is distributed in the shallow part of outer-rise region including the rupture area of Event 2. Therefore, we conclude that Event 2 was triggered by Event 1.

Keywords: outer-rise earthquake, tele-seismic body-wave analysis, coseismic slip distribution, dCFF

Japan Geoscience Union Meeting 2013
(May 19-24 2013 at Makuhari, Chiba, Japan)

SSS28-P13 Room:Convention Hall Time:May 23 18:15-19:30

Rupture Process of Moderate-Size Earthquakes by the MeSO-net

Ko Nishizawa[1], Takumi Murakoshi[1*], Yasuyuki Iwase[1], Takao Eguchi[1], Shin'ichi Sakai[1], Shigeki Nakagawa[2], Naoshi Hirata[2], Ryou Honda[3], Hisanori Kimura[4]

[1]National Defense Academy, [2]ERI, Univ. of Tokyo, [3]Hot Springs Research Institute of Kanagawa Prefecture, [4]NIED

The purpose of this study is to obtain the rupture process of moderate-size earthquakes in space and time by using waveforms in the Metropolitan Seismic Observation Network (MeSO-net). The MeSO-net is high-density seismograph network in and around the Tokyo metropolitan area, Japan. About 300 seismic stations are installed in the average intervals of several kilometers.The average station-to-station distance in MeSO-net is less than a quarter of existing seismic networks in Japan, where the average distances in K-net and KiK-net are about 20 km. In this study, we analyzed the fault motion of moderate-size earthquakes in and around Kanto region, Japan by applying the back-projection method to seismic waveforms in MeSO-net. We obtained detail images of the rupture process of moderate-size earthquakes.

Keywords: back-projection method, rupture process, MeSO-net, moderate-size earthquake

Japan Geoscience Union Meeting 2013
(May 19-24 2013 at Makuhari, Chiba, Japan)

SSS28-P14 Room:Convention Hall Time:May 23 18:15-19:30

Estimation of Radiated Seismic Energy from Regional and Teleseismic Waveforms

Ryota Kiuchi[1*], MORI, James[1]

[1]DPRI, Kyoto University

Therefore, it is important to compare different methods for estimating the radiated energy. Especially, we are interested in studying the apparent stress (rigidity multiplied by the ratio between radiated energy and seismic moment) of strike-slip earthquakes in the oceanic lithosphere, because it is often high (Choy and McGarr, 2002). However, this result is obtained from teleseismic P waves, and it is often difficult to correct for the radiation pattern of nodal arrivals, therefore, the estimated apparent stress may have a large variations.

In this study, we estimated the radiated energy for two large strike-slip earthquakes in Japan, the 2000 western Tottori earthquake (Mw 6.7) and the 2005 West off Fukuoka Prefecture earthquake (Mw 6.6), using both regional (less than 100km) and teleseismic (30deg $<$ delta $<$ 90deg) waveforms. To estimate the energy correctly, it is necessary to account for source effects (e.g.,radiation pattern) and path effects (e.g.,attenuation). We use only P waves for the teleseismic waveform, because of the strong attenuaion of teleseismic S waves and interference with other phases. For the teleseismic waveforms we need to account not only direct P but also depth phase, pP and sP (Boatwright and Choy, 1986).

The results show that the radiated energy of two earthquakes are not high. We will examine the each data carefully, and evaluate the differences in results from the different teleseismic and locally recorded data.

Keywords: radiated energy, apparent stress, strike-slip earthquake

Japan Geoscience Union Meeting 2013
(May 19-24 2013 at Makuhari, Chiba, Japan)

SSS28-P15 Room:Convention Hall Time:May 23 18:15-19:30

Aftershocks Properties of the 2010 ML 6.4 Jiashian earthquake in Southern Taiwan

Chi-Chia Tang[1*], Cheng-Horng Lin[1]

[1]Institute of Earth Sciences, Academia Sinica

Large earthquakes often occur in unexpected locations and are followed by numerous aftershocks. Nevertheless, the aftershock properties of large earthquakes are not usually discovered in detail because a significant portion of aftershock sequences is missing in existing earthquake catalogues, mainly due to overlapping arrivals of seismic waves from these events. We examined waveform data of aftershocks of the 2010 ML 6.4 Jiashian earthquake recorded by the 19 stations of the Central Weather Bureau Seismic Network. We utilize a matched filter technique which Peng and Zhao (2009) used in detecting early aftershocks to discovery missing aftershocks. We use waveforms of 574 aftershocks as templates and scanned three-day data since the original time of mainshock. We identify ~ 4 times more aftershocks than listed in the catalogue of Central Weather Bureau. We find that newly detected events mainly concentrated within first 24 hours and most of them occurred with magnitudes < 2.0. The aftershocks migrated westward from the epicenter of mainshock, ~ 90 degree counterclockwise from the trend of adjacent faults. The seismicity rate of detected aftershocks is proportional to the inverse of time since the mainshock following the Omori Law.

Keywords: Aftershock, Jiashian, Taiwan

Japan Geoscience Union Meeting 2013
(May 19-24 2013 at Makuhari, Chiba, Japan)

SSS28-P16 Room:Convention Hall Time:May 23 18:15-19:30

An Adjoint Data Assimilation Method for Optimizing Frictional Parameters on the Afterslip Area

Masayuki Kano[1*], Shin'ichi Miyazaki[1], Kosuke Ito[2], Kazuro Hirahara[1]

[1]Kyoto Univ., [2]JAMSTEC

Afterslip sometimes triggers another earthquake in the time-scale of days to several years. Thus it may be possible to predict the occurrence of such a triggered earthquake by simulating the spatio-temporal evolution of afterslip with the estimated frictional parameters. To demonstrate the feasibility of this idea, we consider a plate interface model where afterslip propagates between two asperities following a rate and state friction law and adopt an adjoint data assimilation method to optimize frictional parameters. Synthetic observation data are sampled as the slip velocities on the plate interface during 20 days. It is found that 1) all frictional parameters are optimized if data set consist not only of the early phase of afterslip or acceleration, but also of decaying phase or deceleration and 2) that the prediction of the timing of the triggered earthquake is improved by using adjusted frictional parameters.

Keywords: afterslip, frictional parameters, data assimilation

Japan Geoscience Union Meeting 2013
(May 19-24 2013 at Makuhari, Chiba, Japan)

SSS28-P17 Room:Convention Hall Time:May 23 18:15-19:30

Source Parameter Study of Hydraulic Fracturing induced Microearthquakes using Empirical Green's functions

Ahyi KIM[1*], IIDA, Shuhei[1], RUTLEDGE, James[2]

[1]Yokohama City University, [2]Schlumberger

Hydraulic fracturing is a technique used to allow economic production of gas and oil from low-permeability reservoirs. The technique is also used to enhance geothermal energy development. Currently, microseismicity induced by the fluid injection is routinely monitored to map the fracture growth process in real-time. A natural development is to characterize the mechanism of the microearthquakes. Understanding source characteristics of these events is expected to provide a better understanding of the fracturing process and the influence of pre-existing structures controlling the distribution of events. Although several focal mechanism studies have been done in gas and geothermal field, its estimation is often biased due to various errors. Often the most significant difficulty in retrieving the source parameters in these monitoring studies is from poor azimuthal coverage. To avoid these uncertainties in this study, we estimate the source parameters using the empirical Green's function (eGf) analysis. The eGf approach is advantageous because it can be performed with one receiver, and requires no assumption of geologic model. We deconvolve the smaller event from the larger events recorded at the same receiver to obtain the source time functions of the larger events. We use the source-time functions to fit the seismic moment and corner frequency of the source-time spectra using a least-squares curve fit to the f2 spectra. The data we use were recorded during a hydraulic fracture imaging test in the Carthage Cotton Valley gas field of east Texas using two multi-level, three-component geophone arrays deployed in nearby monitoring wells. The treatments monitored include gel-proppant treatments using high viscosity fluids and low-viscosity water frac treatments In this study we apply the eGf method to the events precisely relocated from two injection stages ($-2.4 < Mw < -0.6$). Preliminary result indicates source spectra of most events agree well with double couple event. We also examine the correlation of the corner frequency and seismic moment to investigate whether those events follows the self-similarity observed in tectonic events.

Keywords: Hydraulic fracturing, Microearthquakes, Empirical Green's function, Source spectra, Source characteristics, Scaling Law

Japan Geoscience Union Meeting 2013
(May 19-24 2013 at Makuhari, Chiba, Japan)

SSS28-P18 Room:Convention Hall Time:May 23 18:15-19:30

AE in rock under triaxial compression with small perturbation of confining pressure - Comparison with b-value variation-

Takashi Satoh[1*], Xinglin Lei[1]

[1]GSJ/AIST

It is well known that seismic activity may be affected by small perturbation of crustal stress such as earth tide. Tanaka (2010, 2012) showed that the correlation between tidal stress and earthquake occurrence time had became significant since about 10 years before the 2004 Sumatra earthquake (Mw9.0) and 2011 Tohoku-oki earthquakes (Mw9.1), and it disappeared after the main shocks. The correlation was the highest around the hypocenter regions of these earthquakes. Nanjo et al. (2012) found similar space-time variation patterns of the b-value in Gutenberg-Richer frequency magnitude relation before and after these earthquakes.

In order to study effects of small stress perturbation on seismic activity, we have measured acoustic emissions (AEs) during triaxial compression experiments with small periodic perturbation of confining pressure (Pc). We reported so far experiments using granite samples drilled near the Nojima fault (Satoh & Lei, 2010), and that using a Westerly granite sample having artificial defects (Satoh & Lei, 2012). In this report, motivated by Nanjo et al. (2012), we compared the changes in the correlation between AE activity and Pc perturbation observed in these experiments with the b-value variation. It seems that the higher correlation between AE activity and Pc perturbation corresponds to the lower b-value, which is consistent with what observed for the M9 class earthquakes reported by Tanaka (2010, 2012) and Nanjo et al. (2012).

<References>
Nanjo et al., 2012, GRL, vol.39, L20304, doi:10.1029/2012GL052997.
Satoh & Lei, 2010, Seism. Soc. Japan, 2010 Fall Meeting, C11-04.
Satoh & Lei, 2012, Seism. Soc. Japan, 2012 Fall Meeting, D31-3.
Tanaka, 2010, GRL, vol.37, L02301, doi:10.1029/2009GL041581.
Tanaka, 2012, GRL, vol.39, L00G26, doi:10.1029/2012GL051179.

Keywords: Small periodic stress perturbation, AE activity, b-value

Japan Geoscience Union Meeting 2013
(May 19-24 2013 at Makuhari, Chiba, Japan)

SSS28-P19 Room:Convention Hall Time:May 23 18:15-19:30

A detailed view of the injection-induced seismicity in a carbonate gas reservoir in Southwestern Sichuan Basin, China

Xinglin Lei[1*], Shengli Ma[2], Wenkang[3], Chunmei Pang[3], Jie Zeng[3], Bing Jiang[3]

[1]Geological Survey of Japan, AIST, Japan, [2]Institute of Geology, China Earthquake Administration, [3]Zigong Earthquake Administration

Seismicity at a gas reservoir located in the relatively stable Sichuan Basin, China, mirrors the injection pressure of unwanted water, suggesting that the seismicity is injection induced. Injection under high pressure on a routine basis began on 9 Jan. 2009, and continued to July 2011. During the injection period, over 120,000 m^3 of water was pumped under a wellhead pressure of up to 6.2 MPa into the limestone formation of Permian 2.45 to 2.55 km beneath the surface. The injection induced more than 7,000 surface recorded earthquakes, including 2 M4+ (the largest one was ML4.4), 20 M3+, and more than 100 M2+ events. Data observed by a nearby local seismic network and five temporal stations provide a detailed view of the spatio-temporal distribution of the induced earthquakes. Most events were limited to depths ranging from 2.5 to 3.5 km, which is consistent with the limestone formation of Permian. In a map view, hypocenters are concentrated in a NNW extended ellipsoidal zone approximately 6 km long and approximately 2 km wide centered approximately 1 km northwest of the injection well.

The spatio-temporal distribution and other statistical results indicate that the triggered seismicity is characterized by four typical phases, which reflect the patterns of the injection rate and wellhead pressure. The largest ML4.4 events occurred when the wellhead pressure reached 0.9 MPa at the very beginning of injection. Various factors, such as the shear mechanism, the pattern of hypocenter distribution, and the fractal dimensions, indicate that the induced seismicity in the region resulted from the reactivation of pre-existing faults. Injected fluids diffuse outward along pre-existing faults, which were originally stressed, weakening the faults and leading to their reactivation. The intersections of a set of conjugate fractures are particularly suitable for fluid flowing. Some relatively large dipped faults likely bound the outward fluid flow and provide paths for upward leakage and downward flow.

The overall migration front follows a typical pore-pressure diffusion curve with a hydraulic diffusivity of 0.1 m^2/s. There are also some fast responses of seismicity on pressure change reflecting pore-pressure diffusion along the surface of pre-existing faults with a hydraulic diffusivity on the order of 1 to 10 m^2/s. Multi sources of evidence, such as the shear mechanism, pattern of hypocenter distribution, and small elevated pore pressure as compared with the least principal stress in the region show that the induced earthquakes occurred as a result of lowering of the effective normal stress on known or unknown pre-existing blind faults.

Keywords: Injection-induced seismicity, Gas field, Carbonate Reservoir, ETAS model, Pore-pressure

Japan Geoscience Union Meeting 2013
(May 19-24 2013 at Makuhari, Chiba, Japan)

SSS28-P20 Room:Convention Hall Time:May 23 18:15-19:30

In-situ stress measurement at the closest proximity of an M1.5 earthquake at Tau Tona gold mine in South Africa

Hiroshi Ogasawara[1*], Gerhard Hofmann[2], Harumi Kato[3], Chris Stander[2], Gilbert Morema[4], Trevor Clements[5], Phil Piper[5]

[1]College of Science and Engineering, Ritsumeikan University, [2]Anglogold Ashanti Ltd. Rock Engineering, [3]Akema Boring Ltd., [4]Seismogen CC, [5]Ground Work Ltd.

In-situ stress measurements were successfully carried out in close proximity to a M1.5 damaging seismic event at 104 level (about 2950 m depth) at Tau Tona gold mine in South Africa. This event occurred on 3 December 2012, and on the 6th and 7th of February 2013, three overcoring stress measurements were done. The seismic event took place almost at the end of a pilot tunnel (see a photo attached), and significant dynamic rock mass ejection from the sidewall of the tunnel occurred. Elastic numerical modelling did not indicate any anomalous stress levels, but due to the severity of the damage it was important to better understand prevailing stress conditions. Stress measurement methods commonly used in South Africa (e.g. CSIR triaxial cell method or CSIRO HI method) was not suitable for such high stress conditions or adverse drilling conditions.

We used the BX CCBO technique (60mm diameter CCBO overcoring), a downsized version of the Compact Conic Borehole-end Overcoring technique (76mm diameter overcoring; Sakaguchi et al. 1992; Sugawara and Obara 1999; ISRM suggested). For overcoring, 6-15m BX pilot holes are drilled from tunnels at depths. Tools are used allowing implementation of the technique for typical South African geological drilling setups with small pneumatic machines. The procedure was first proven effective in South African gold mine conditions in 2011, on 98 L at Moab Khotsong Mine (about 3.0km depth) at an area with supposed minimal mining perturbation (Ogasawara et al. J. SAIMM 2012) . The technique was also implemented on 28 and 29th of January 2013 at Mponeng Gold Mine, 120L (an about 3350 m depth) also at an area with least mining stress perturbation.

At both the 3.0km-deep site at Moab Khotsong mine and the 3.4km-deep site at Mponeng mine, the measured maximum principal stress was consistent with overburden pressure. The determined orientations of intermediate principal stress (the horizontal maximum principal stress) and its ratio to the maximum principal stress was also consistent with the stress fields that well accounted for the fault slip mechanisms of nearby M2-4 earthquakes in the mines (e.g. Hofmann and Murphy 2007; Hofmann and Scheepers 2010).

At the moment, we have to wait for lab test for elastic modulus of the cores recovered from the measurement hole. However, if we used a typical elastic modulus for the lithology of the site, the measured stress at 104L (about 3.0km depth with least mining) at Tau Tona was much larger than the measured stress at 120L (a 3.4km depth with least mining) at Mponeng mine.

No in-situ stress measurements have been carried out close to the area of the damaging seismic event before, and hence no stress information was available towards mitigating seismic risk. It was proven that the BX CCBO technique can be implemented in adverse underground conditions - high stress and limited shift working hours in the South African gold mines. We hope that stress measurement can be done regularly together with a pilot geological drilling program, prior to advancing the pilot tunnel, which will fundamentally contribute to mitigate seismic risk in South African gold mines.

We were very much encouraged to make additional plans to see more detailed of stress distribution of seismic sources in South African gold mines.

These measurements were funded by JST-JICA SATREPS and Anglogold Ashanti Ltd.

Photo. The M1.5 seismic damage at a pilot tunnel at 104L at Tau Tona, at the closest proximity of which the BX CCBO in-situ stress measurement was carried out. Harumi Kato and Gerhard Hofmann look at a potential rupture plane on the side wall. Photo by Hiroshi Ogasawara.

Keywords: In-situ stress measurement, Closest proximity of a hypocenter, South African gold mine, BX CCBO technique

SSS28-P20 Room:Convention Hall Time:May 23 18:15-19:30